NANO LETTERS

Subscriber access provided by HARVARD UNIV

Letter

Coaxial Group III#Nitride Nanowire Photovoltaics

Yajie Dong, Bozhi Tian, Thomas J. Kempa, and Charles M. Lieber

Nano Lett., **2009**, 9 (5), 2183-2187• Publication Date (Web): 21 April 2009

Downloaded from http://pubs.acs.org on May 13, 2009

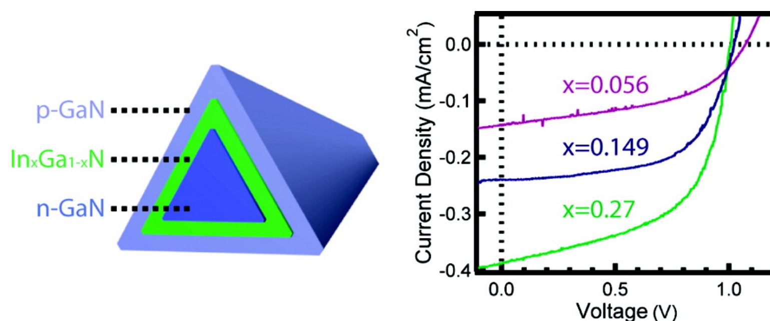

More About This Article

Additional resources and features associated with this article are available within the HTML version:

- Supporting Information
- Access to high resolution figures
- Links to articles and content related to this article
- Copyright permission to reproduce figures and/or text from this article

View the Full Text HTML

ACS Publications
High quality. High impact.

Nano Letters is published by the American Chemical Society. 1155 Sixteenth Street N.W., Washington, DC 20036

NANO LETTERS

2009
Vol. 9, No. 5
2183-2187

Coaxial Group III−Nitride Nanowire Photovoltaics

Yajie Dong,[†] Bozhi Tian,[†] Thomas J. Kempa,[†] and Charles M. Lieber*[,†,‡]

Department of Chemistry and Chemical Biology and School of Engineering and Applied Sciences, Harvard University, Cambridge, Massachusetts 02138

Received March 17, 2009; Revised Manuscript Received April 12, 2009

ABSTRACT

Coaxial core/shell nanowires represent an important class of nanoscale building blocks with substantial potential for exploring new concepts and materials for solar energy conversion. Here, we report the first experimental realization of coaxial group III−nitride nanowire photovoltaic (PV) devices, n-GaN/i-$In_xGa_{1-x}N$/p-GaN, where variation of indium mole fraction is used to control the active layer band gap and hence light absorption. Current−voltage data reveal clear diode characteristics with ideality factors from 3.9 to 5.6. Electroluminescence measurements demonstrate tunable emission from 556 to 371 nm and thus confirm band gap variations in the $In_xGa_{1-x}N$ active layer from 2.25 to 3.34 eV as In composition is varied. Simulated one-sun AM 1.5G illumination yielded open-circuit voltages (V_{oc}) from 1.0 to 2.0 V and short-circuit current densities (J_{sc}) from 0.39 to 0.059 mA/cm^2 as In composition is decreased from 0.27 to 0 and a maximum efficiency of ∼0.19%. The n-GaN/i-$In_xGa_{1-x}N$/p-GaN nanowire devices are highly robust and exhibit enhanced efficiencies for concentrated solar light illuminations as well as single nanowire J_{sc} values as high as 390 mA/cm^2 under intense short-wavelength illumination. The ability to rationally tune the structure and composition of these core/shell III−nitride nanowires will make them a powerful platform for exploring nanoenabled PVs in the future.

Inorganic nanostructures, such as nanoparticles, nanorods, and nanowires, are currently under active investigation as components for photovoltaic (PV) devices due to their potential for exploring new device concepts and increasing the efficiency of low-cost solution processed solar cells.[1−15] Nanostructures have been employed to improve charge collection efficiency in dye-sensitized[3,4] and polymer blend solar cells,[5] and to investigate carrier multiplication.[8,9] However, solar cells based on inorganic/organic hybrid nanoarchitectures often suffer from relatively low efficiencies and poor stabilities compared to all inorganic cells and, to date, have not been investigated as integrated power sources for nanoelectronics.

Recently, semiconductor nanowires have emerged as building blocks for PV devices, where studies have investigated fundamental device performance limits in several different nanowire structural motifs.[10−15] We have reported studies of p-type/intrinsic/n-type (p−i−n) dopant modulation in coaxial[11] and axial[13,14] silicon nanowires and have shown functional PV devices configured at the single nanowire level with J_{sc} and efficiencies up to 23.9 mA/cm^2 and to 3.4%, respectively, under 1-sun AM 1.5G illumination.[11] Alternatively, rectifying metal contacts to unintentionally doped silicon nanowires have been used to define single nanowire PVs with 1-sun J_{sc} and efficiency values of ∼5.0 mA/cm^2 and 0.5%, respectively.[15] Interestingly, individual nanowire PV elements can be interfaced with and provide power for nanoelectronics which consume power at the nanowatt scale.[11,14]

Most previous nanowire PV research has focused on silicon nanowires whose doping and morphology can be readily controlled,[11,13,14] although the indirect band gap of silicon can limit light absorption in nanoscale. In contrast, group III nitrides have attracted considerable attention as potential full-solar-spectrum PV materials since the band gap of $In_xGa_{1-x}N$ can in principle be tuned to span nearly the entire solar spectrum from 0.7 to 3.4 eV.[16−18] Extensive research focused on the growth of III−nitride thin films on (lattice mismatched) sapphire substrates[19,20] has shown relatively high densities of threading dislocations, which unfortunately degrade p−n diode device performance by increasing leakage current.[21]

In contrast, the synthesis of III−nitride nanowires can be virtually substrate-free, which prevents the formation of dislocations originating from lattice mismatch between nanowires and the planar growth substrate.[22−28] Moreover, the effective relaxation of lateral strain in coaxial heterostructured nanowires can enable high-quality integration of materials with larger lattice mismatches than possible in traditional planar structures.[22,29] Coaxial III−nitride nanowires have been shown to be dislocation-free single crystals.[22−27] In addition, successful doping and composition modulation of these nanowires have led to demonstrations of multicolor, high-efficiency light emitting diodes (LEDs),[23,24] lasers,[25,26] and high electron mobility transistors

* Corresponding author, cml@cmliris.harvard.edu.
[†] Department of Chemistry and Chemical Biology.
[‡] School of Engineering and Applied Sciences.

10.1021/nl900858v CCC: $40.75 © 2009 American Chemical Society
Published on Web 04/21/2009

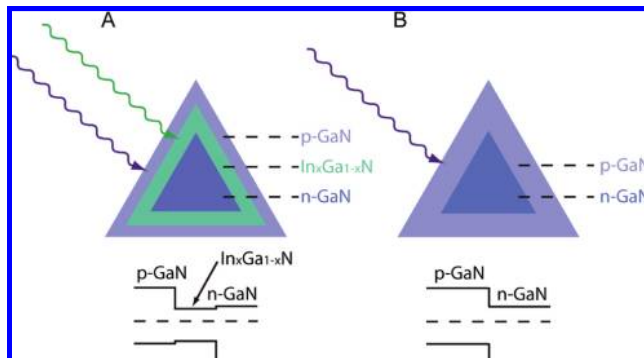

Figure 1. Cross-sectional view of (A) p-GaN/i-In$_x$Ga$_{1-x}$N/n-GaN heterojunction and (B) p-GaN/n-GaN homojunction nanowire structural motifs and their corresponding energy band diagrams. The wavy colored arrows in the cross-section view indicate light of different wavelengths that is absorbed by the nanowires. The dashed lines in the band diagrams indicate the position of the Fermi level.

(HEMTs)[27] and thus suggest that coaxial core/shell III−nitride nanowire motif could provide unique opportunities for PVs.

We have focused on n-GaN/i-In$_x$Ga$_{1-x}$N/p-GaN core/shell/shell nanowire structures illustrated in Figure 1A. A key advantage of this core/shell/shell architecture is that the p−i−n interface extends along the entire length of the nanowire with carrier separation in the radial direction, as discussed previously for p−i−n coaxial Si nanowires.[11,14] In this geometry, photogenerated carriers can reach the p−i−n junction with high efficiency since diffusion lengths are relatively short. The direct and tunable band gap of i-In$_x$Ga$_{1-x}$N alloys leads to a large absorption coefficient of approximately 10^5 cm^{-1} at the band edge.[30] Hence, >85% of the incident light with energy above the band gap, which can be tuned with the value of x, can be absorbed within the first 200 nm of material. We also designed and studied control structures with $x = 0$ (Figure 1B) as part of these studies since In incorporation in In$_x$Ga$_{1-x}$N alloy may reduce crystal quality due to strain and inhomogeneity.[31] All of the coaxial nanowire heterostructures were synthesized by metal−organic chemical vapor deposition (MOCVD), using a strategy involving axial elongation by nanocluster catalyzed growth followed by controlled shell deposition onto the nanowire core as described previously.[22−27,32] The indium composition was systematically tuned to define the band gap of InGaN by adjusting the InGaN shell growth temperature.[31,32]

To characterize electrical transport through the coaxial n-GaN/i-In$_x$Ga$_{1-x}$N/p-GaN nanowires, we fabricated metal contacts selectively to the inner n-core and outer p-shell as shown schematically in Figure 2A. Briefly, the nanowires were etched using inductively coupled plasma reactive ion etching (ICP-RIE) to expose the n-core in a lithographically defined region at one end, and then metal contacts were made to the n-core and p-shell separately after additional lithographic patterning steps.[33] At least 10 devices were studied for each nanowire growth condition. A scanning electron microscopy (SEM) image of a typical device fabricated in this way (Figure 2B) shows a smooth morphology in the etched region, suggesting good etch uniformity and low ion damage during the ICP-RIE processing.[34] The estimated depth of the ICP-RIE etch, ~240 nm, was adjusted to exceed slightly the total thickness of the coaxial i-In$_x$Ga$_{1-x}$N/p-GaN shells. In addition, the SEM image demonstrates clearly the formation of metal contacts selectively to the etched n-core and outer p-shell of the coaxial n-GaN/i-In$_x$Ga$_{1-x}$N/p-GaN nanowire.

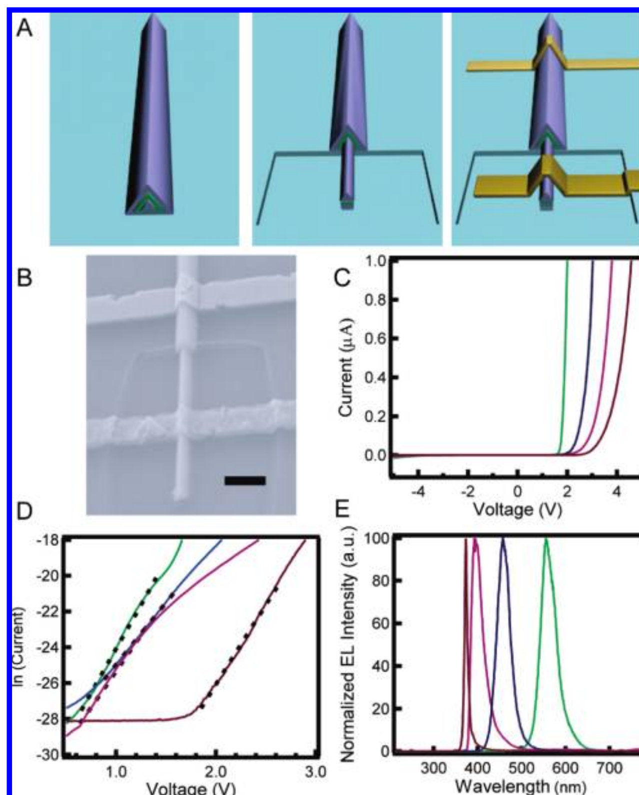

Figure 2. Device fabrication and characterizations. (A) Schematics of device fabrication: left, coaxial n-GaN/i-In$_x$Ga$_{1-x}$N/p-GaN nanowire heterostructures; middle, exposed the n-core at nanowire end following ICP-RIE etch; right, Ni/Au and Ti/Al/Ti/Au metal contacts deposited on the p-shell and n-core, respectively. (B) SEM image of a representative nanowire device. Scale bar is 2 μm. (C) Dark $I-V$ curves of three heterojunction nanowires (from left to right, denoted with green, blue and purple color with increasing InGaN layer growth temperature 715, 745, and 775 °C) and one homojunction ($x = 0$) nanowire (denoted with dark violet color). (D) Semilog scale $I-V$ curves, where the ideality factor and dark saturation current are extrapolated from the linear regimes (dashed lines). (E) Normalized electroluminescence spectra recorded from the four devices characterized in Figure 2C.

Dark current−voltage ($I-V$) curves collected from three representative n-GaN/i-In$_x$Ga$_{1-x}$N/p-GaN nanowires, which were synthesized with the InGaN shell growth temperature varied from 775 to 715 °C, and an $x = 0$ n-GaN/p-GaN control nanowire (Figure 2C) exhibit several notable features. First, the $I-V$ data for the four representative nanowires all show well-defined rectifying behavior characteristic of a diode structure. $I-V$ curves recorded across the p- or n-segments alone in nanowire devices containing multiple contacts showed symmetrical behavior,[23] thus confirming that current rectification is due to the built-in electric field across the p−n junction. Second, the turn-on voltages for these

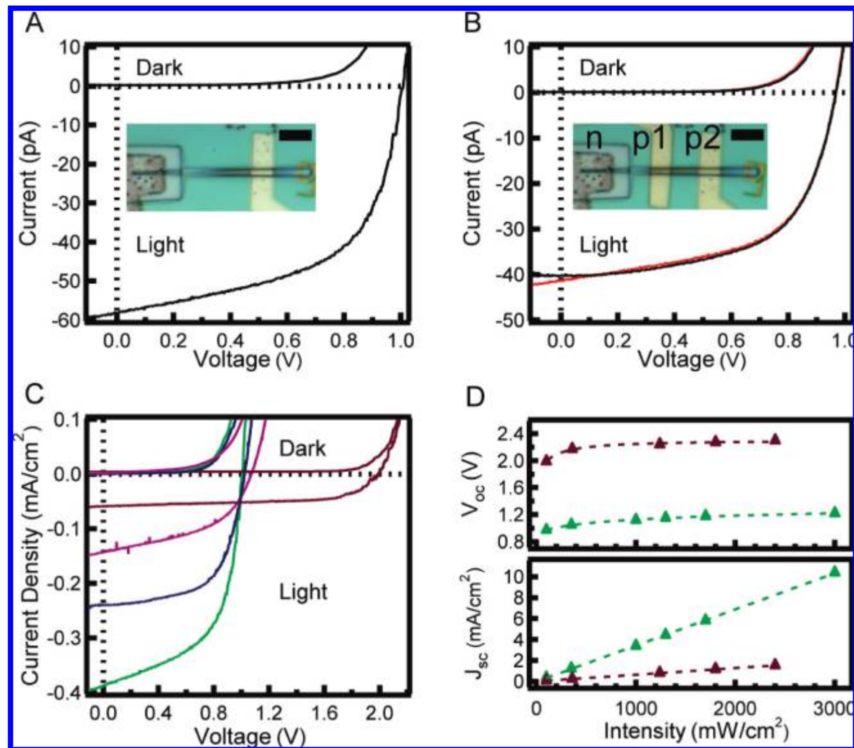

Figure 3. Characterization of the nanowire photovoltaic devices under solar illumination. (A) Light $I-V$ curves for a green PV device. Inset, optical microscopy image of the device; scale bar is 5 μm. (B) Light $I-V$ curves for p1−n and p2−n contact configuration for same device as in (A). Inset, optical image of the nanowire device; scale bar is 5 μm. (C) Dark and light $J-V$ curves of representative ultraviolet, purple, blue, and green nanowire PV devices. (D) Light intensity dependent on J_{sc} and V_{oc} for representative ultraviolet (dark violet triangles) and green (green triangles) devices. Lines through the V_{oc} and J_{sc} data correspond to guides to logarithmic and linear dependencies, respectively.

diodes from 1.82 to 3.28 V concomitant with the InGaN layer growth temperature increase from 715 to 775 °C. This is consistent with a controlled increase in the InGaN layer band gap that is expected and previously documented with decreasing indium composition at higher growth temperatures.[31] As a limiting case, the n-GaN/p-GaN control device shows the maximum turn-on voltage of ca. 3.90 V. Fits to the linear regions of ln(I)−V data of these diodes (Figure 2D) yield diode ideality factors n and dark saturation current I_0.[35] The ideality factor values range between 3.9 and 5.6. This is consistent with planar III−nitride diodes in which anomalously high ideality factors up to 7 were experimentally observed.[36] Interestingly, the dark saturation current of n-GaN/p-GaN control nanowire is only 9×10^{-5} fA, approximately 10^5 times lower than that of the three n-GaN/i-$In_xGa_{1-x}N$/p-GaN devices ($x > 0$), for which I_0 ranges from 2 to 14 fA. This comparison of I_0 values indicates a superior crystal quality of these control devices and, correspondingly, that improvements could be obtained in the future by further optimizing the InGaN layer.

To probe directly the band gap of the active InGaN layer of n-GaN/i-$In_xGa_{1-x}N$/p-GaN nanowire diodes, we characterized electroluminescence (EL) in forward biased devices. Normalized EL spectra (Figure 2E) collected from the four devices shown in Figure 2C exhibited luminescence maxima at 556, 457, 396, and 371 nm; for simplicity, we denote these devices as green, blue, purple, and ultraviolet (UV) in the following discussion. The wavelengths of green, blue, and purple cells are consistent with band-edge emission from $In_xGa_{1-x}N$ with In compositions of ca. 27, 14.9, and 5.6%, respectively,[37] while the 371 nm emission of the UV cell corresponds to the n-GaN/p-GaN homojunction band-edge radiative recombination. In addition, measurement of the full width at half-maximum of these spectra yields values of 40, 34, 30, and 7 nm, respectively. The broadening with increasing In concentration is consistent with InGaN-based thin film LEDs[31] and can be attributed to increasing strain and/or phase separation as the In composition is increased. Overall, these results demonstrate that the InGaN band gaps of our n-GaN/i-$In_xGa_{1-x}N$/p-GaN nanowire structures, which will dictate the absorption properties of devices, can be readily tuned through In composition control during nanowire growth.

The photovoltaic properties of these coaxial n-GaN/i-$In_xGa_{1-x}N$/p-GaN nanowire devices were first characterized under 1-sun (AM 1.5G) illumination. $I-V$ data recorded from a representative green cell (Figure 3A) yields an open-circuit voltage, V_{oc}, of 1.0 V, a short-circuit current, I_{sc}, of 58 pA, and a fill factor, FF, of 56%. Notably, the open-circuit voltage is much larger than what has been achieved before with Si nanowires (∼0.3 V)[11,13] and is one of the highest values of all nanoenabled solar cells. However, the short-circuit current remains much lower than the best value obtained with single Si nanowire devices (∼500 pA). To probe whether the relatively large p-type GaN series resistance has a negative effect on the photocurrent collection, we fabricated one

additional p-contact on this device. $I-V$ data recorded using contacts to the p-shell that were 6.1 μm (p1) and 13.1 μm (p2) from the n-core contact (Figure 3B) exhibited essentially the same V_{oc} and less than 2.5% difference in I_{sc}, thus indicating that the p-shell is equipotential with radial carrier separation occurring uniformly along the entire length of the core/shell nanowire device. Hence, the low short-circuit current is most likely a consequence of lower light absorption and carrier generation and not of poor carrier collection, although interfacial and/or surface recombination may also contribute.

A comparison of I_{sc} for the device with one and two p-shell contacts in parts A and B of Figure 3, respectively, also shows that I_{sc} drops by ~28% with the similar decrease in projected nanowire area; that is, only the exposed coaxial n-GaN/i-$In_xGa_{1-x}N$/p-GaN nanowire regions contribute substantially to the photocurrent. This is consistent with our previous results for p−i−n coaxial Si nanowires[11] and indicates that the exposed area can be used to obtain an upper limit estimate of the current density, J. $J-V$ data calculated in this manner for representative green, blue, purple, and UV nanowire devices (Figure 3C) yield V_{oc} and J_{sc} values of 1.0 V and 0.39 mA/cm^2, 1.0 V and 0.24 mA/cm^2, 1.1 V and 0.14 mA/cm^2, and 2.0 V and 0.059 mA/cm^2, respectively. The results show a systematic increase in V_{oc} and decrease in J_{sc} from green to UV cells. Qualitatively, the increase in V_{oc} is consistent with the band gap increase upon decreasing In composition, while the decrease in J_{sc} is a result of a reduced carrier generation as a diminishing portion of the solar spectrum becomes available for absorption with increasing band gap. The substantially larger V_{oc} determined for the n-GaN/p-GaN versus n-GaN/i-$In_xGa_{1-x}N$/p-GaN nanowire devices suggests that improvements in V_{oc} could be achieved by optimizing the InGaN material growth in the future.

We have also investigated the light intensity dependence of the output properties to characterize further the potential of the n-GaN/i-$In_xGa_{1-x}N$/p-GaN nanowire devices. J_{sc} and V_{oc} data for the limiting cases of $x = 0.27$ and 0 with illumination intensities from 1 to 30 suns (Figure 3D) show linear (J_{sc}) and logarithmic (V_{oc}) increases with increasing intensity as expected for a PV diode structure.[35] The green cell consistently exhibits J_{sc} values ~6 times higher than those obtained for the UV cell. These data can be attributed to the smaller InGaN band gap of ~2.23 eV, which allows the green cell to absorb ~20% versus <2% of solar photons for the UV device. With 30 suns illumination, the J_{sc} and V_{oc} for the green cell can be as high as 10.4 mA/cm^2 and 1.22 V, respectively, bringing the apparent energy conversion efficiency from 0.19% at 1 sun to 0.25%. Significantly, all of the n-GaN/i-$In_xGa_{1-x}N$/p-GaN PV devices exhibit no observable degradation after 30 sun illumination for measurements made over a half year. These results thus demonstrate excellent robustness and stability for our fully integrated inorganic nanowire photovoltaic elements under intense illumination, a feature distinct from hybrid systems utilizing organic dyes or polymers with inorganic nanostructures and one that might open up opportunities in concentration solar cells.

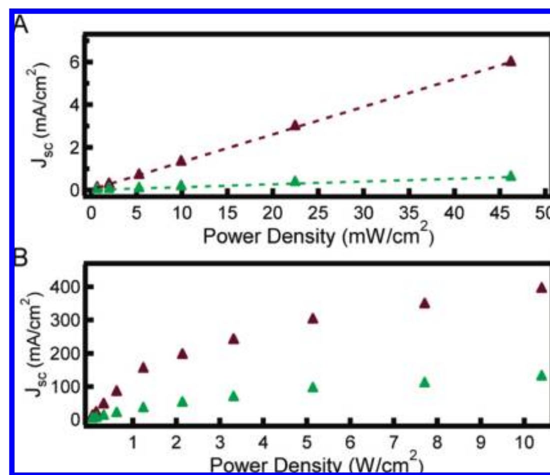

Figure 4. J_{sc} vs power density for low (A) and high (B) average power density conditions (266 nm laser illumination). Dashed lines through data in (A) are guides to highlight the linear dependence for both devices.

To further explore the robustness of the n-GaN/i-$In_xGa_{1-x}N$/p-GaN nanowire design and its potential for operating under highly concentrated illumination, we have characterized the output characteristics under UV laser illumination.[33] The J_{sc} data for UV and green cells recorded with increasing laser illumination intensities (Figure 4) show several important features. As expected, both cells show higher J_{sc} under UV illumination than under solar spectrum illumination of the same power density since the 266 nm/4.66 eV light is fully absorbed by both green and UV nanowire devices with band gaps of 2.23 and 3.4 eV, respectively. Notably, illumination with a power density of 10.4 W/cm^2 yielded a J_{sc} of ~390 mA/cm^2 for the n-GaN/p-GaN nanowire PV device. This suggests substantial promise for high-power n-GaN/i-$In_xGa_{1-x}N$/p-GaN nanowire PV devices by tuning the InGaN layer to overlap better with the solar spectrum. In addition, the J_{sc} data exhibit expected linear dependence on intensity[35] below 50 mW/cm^2, although data begin to saturate for higher power densities. We attribute this nonideal behavior to series resistance contribution from the nonideal p-type contact and believe that PV response could be further improved by optimizing the p-shell and p-shell/contact resistances.

In summary, we have demonstrated the first experimental realization of coaxial III−nitride nanowire PV devices, n-GaN/i-$In_xGa_{1-x}N$/p-GaN, where variation of indium mole fraction was used to control the active layer band gap and light absorption. Electrical transport data reveal clear diode characteristics with ideality factors from 3.9 to 5.6, and EL measurements further demonstrated band gap tenability of the $In_xGa_{1-x}N$ active layer from 2.25 to 3.34 eV as In composition was varied. Simulated 1-sun AM 1.5G illumination yielded open-circuit voltages (V_{oc}) from 1.0 to 2.0 V and short-circuit current densities (J_{sc}) from 0.39 to 0.059 mA/cm^2 as In composition is decreased from 0.27 to 0 and a maximum efficiency of ~0.19%. The n-GaN/i-$In_xGa_{1-x}N$/p-GaN nanowire devices are highly robust and exhibit enhanced efficiencies for concentrated solar light illuminations as well as single nanowire J_{sc} values as high as 390 mA/cm^2 under intense, short-wavelength illumination. Fur-

ther improvement of the PV properties of our new coaxial core/shell III−nitride nanowires motif will be achievable by improving the crystal quality of the In-rich InGaN layer. In addition, quantum well solar cells,[14] which often could not be realized easily on planar devices due to large lattice mismatch, are possible based on recent demonstration of multi-quantum well InGaN/GaN nanowire structures.[26] We believe that such fundamental studies at the single nanowire level will enable the intrinsic limits of the III−nitride materials system to be defined and that such nanoenabled PV elements hold substantial promise for the development of a new generation of solar energy conversion systems in the future.

Acknowledgment. We thank J. Hu, F. Qian, and Y. Li for helpful discussion. T.J.K. acknowledges support from the NSF Graduate Research Fellowship. C.M.L. acknowledges the Air Force Office of Scientific Research and a contract from MITRE Corporation for support of this work.

References

(1) *Basic Research Needs for Solar Energy Utilization, Report of the Basic Energy Sciences Workshop on Solar Energy Utilization. April 18−21, 2005*; US Department of Energy, Washington, DC, 2005 (http://www.er.doe.gov/bes/reports/abstracts.html#SEU).
(2) Lewis, N. S. *Science* **2007**, *315*, 798.
(3) Gratzel, M. *Nature (London)* **2001**, *414*, 338.
(4) Law, M.; Greene, L. E.; Johnson, J. C.; Saykally, R.; Yang, P. D. *Nat. Mater.* **2005**, *4*, 455.
(5) Huynh, W. U.; Dittmer, J. J.; Alivisatos, A. P. *Science* **2002**, *295*, 2425.
(6) Gur, I.; Fromer, N. A.; Geier, M. L.; Alivisatos, A. P. *Science* **2005**, *310*, 462.
(7) Wu, Y.; Wadia, C.; Ma, W. L.; Sadtler, B.; Alivisatos, A. P. *Nano Lett.* **2008**, *8*, 2551.
(8) Luque, A.; Marti, A.; Nozik, A. J. *MRS Bull.* **2007**, *32*, 236.
(9) McGuire, J. A.; Joo, J.; Pietryga, J. M.; Schaller, R. D.; Klimov, V. I. *Acc. Chem. Res.* **2008**, *41*, 1810.
(10) Kayes, B. M.; Atwater, H. A.; Lewis, N. S. *J. Appl. Phys.* **2005**, *97*, 114302.
(11) Tian, B. Z.; Zheng, X. L.; Kempa, T. J.; Fang, Y.; Yu, N. F.; Yu, G. H.; Huang, J. L.; Lieber, C. M. *Nature (London)* **2007**, *449*, 885.
(12) Tsakalakos, L.; Balch, J.; Fronheiser, J.; Korevaar, B. A.; Sulima, O.; Rand, J. *Appl. Phys. Lett.* **2007**, *91*, 233117.
(13) Kempa, T. J.; Tian, B. Z.; Kim, D. R.; Hu, J. S.; Zheng, X. L.; Lieber, C. M. *Nano Lett.* **2008**, *8*, 3456.
(14) Tian, B. Z.; Kempa, T. J.; Lieber, C. M. *Chem. Soc. Rev.* **2009**, *38*, 16.
(15) Kelzenberg, M. D.; Turner-Evans, D. B.; Kayes, B. M.; Filler, M. A.; Putnam, M. C.; Lewis, N. S.; Atwater, H. A. *Nano Lett.* **2008**, *8*, 710.
(16) Wu, J.; Walukiewicz, W.; Yu, K. M.; Ager, J. W.; Haller, E. E.; Lu, H.; Schaff, W. J.; Saito, Y.; Nanishi, Y. *Appl. Phys. Lett.* **2002**, *80*, 3967.
(17) Davydov, V. Y.; Klochikhin, A. A.; Seisyan, R. P.; Emtsev, V. V.; Ivanov, S. V.; Bechstedt, F.; Furthmuller, J.; Harima, H.; Mudryi, A. V.; Aderhold, J.; Semchinova, O.; Graul, J. *Phys. Status Solidi B* **2002**, *229*, R1.
(18) Wu, J.; Walukiewicz, W.; Yu, K. M.; Shan, W.; Ager, J. W.; Haller, E. E.; Lu, H.; Schaff, W. J.; Metzger, W. K.; Kurtz, S. *J. Appl. Phys.* **2003**, *94*, 6477.
(19) Jani, O.; Ferguson, I.; Honsberg, C.; Kurtz, S. *Appl. Phys. Lett.* **2007**, *91*, 132117.
(20) Neufeld, C. J.; Toledo, N. G.; Cruz, S. C.; Iza, M.; DenBaars, S. P.; Mishra, U. K. *Appl. Phys. Lett.* **2008**, *93*, 143502.
(21) Kozodoy, P.; Ibbetson, J. P.; Marchand, H.; Fini, P. T.; Keller, S.; Speck, J. S.; DenBaars, S. P.; Mishra, U. K. *Appl. Phys. Lett.* **1998**, *73*, 975.
(22) Li, Y.; Qian, F.; Xiang, J.; Lieber, C. M. *Mater. Today* **2006**, *9*, 18.
(23) Qian, F.; Li, Y.; Gradecak, S.; Wang, D. L.; Barrelet, C. J.; Lieber, C. M. *Nano Lett.* **2004**, *4*, 1975.
(24) Qian, F.; Gradecak, S.; Li, Y.; Wen, C. Y.; Lieber, C. M. *Nano Lett.* **2005**, *5*, 2287.
(25) Gradecak, S.; Qian, F.; Li, Y.; Park, H. G.; Lieber, C. M. *Appl. Phys. Lett.* **2005**, *87*, 173111.
(26) Qian, F.; Li, Y.; Gradecak, S.; Park, H. G.; Dong, Y. J.; Ding, Y.; Wang, Z. L.; Lieber, C. M. *Nat. Mater.* **2008**, *7*, 701.
(27) Li, Y.; Xiang, J.; Qian, F.; Gradecak, S.; Wu, Y.; Yan, H.; Blom, D. A.; Lieber, C. M. *Nano Lett.* **2006**, *6*, 1468.
(28) Kuykendall, T.; Ulrich, P.; Aloni, S.; Yang, P. D. *Nat. Mater.* **2007**, *6*, 951.
(29) Lauhon, L.; Gudiksen, M.; Wang, D.; Lieber, C. M. *Nature (London)* **2002**, *420*, 57.
(30) Muth, J. F.; Lee, J. H.; Shmagin, I. K.; Kolbas, R. M.; Casey, H. C.; Keller, B. P.; Mishra, U. K.; DenBaars, S. P. *Appl. Phys. Lett.* **1997**, *71*, 2572.
(31) Nakamura, S.; Pearton, S.; Fasol, G. *The Blue Laser Diode: The Complete Story*; Springer-Verlag: Berlin and Heidelberg, 2000.
(32) Coaxial n-GaN/i-$In_xGa_{1-x}N$/p-GaN core/shell/shell nanowires were synthesized as follows: 0.01 M nickel nitrate solution was deposited on a sapphire substrate and placed in a MOCVD reactor (Thomas Swan Scientific Equipment Ltd.). n-type GaN cores were grown in hydrogen (H_2) at 950 °C and 700 Torr for 4800 s using trimethylgallium (TMG, 22 μmol min^{-1}) and ammonia (NH_3, 67 mmol min^{-1}), while silane (100 ppm in H_2, 2 sccm) was used as the n-type dopant. The intrinsic InGaN layer was sequentially deposited in nitrogen at 715−775 °C and 300 Torr for 500 s, using TMG (5.3 μmol min^{-1}) and trimethylindium (TMI, 6.5 μmol min^{-1}) as Ga and In sources, respectively. Lastly, the p-GaN outer shell was grown in H_2 at 960 °C and 100 Torr for 400 s using bis(cyclopentadienyl)magnesium (MgCp2, 0.65 μmol min^{-1}) as p-type dopant. Our III-nitride nanowires have triangular cross sections, a fact which has been confirmed through HRTEM studies reported previously.[22–27] The triangular side length of the p-i-n nanowires was ca. 1−1.25 μm and the thicknesses of the i-InGaN and p-GaN layers were ca. 80−100 and 100−125 nm, respectively. The lengths of the nanowires after transfer to the substrate for device fabrication were 15 to 40 μm. The coaxial n-GaN/p-GaN core/shell nanowire synthesis was the same as above except that the InGaN layer deposition step was eliminated.
(33) The nanowires were dispersed on silicon substrates (100 nm oxide/200 nm nitride, 1−10 Ω·cm resistivity) for electrical and optoelectronic measurements. Electron beam lithography (EBL) was used to define windows at nanowire ends, and then the shells were etched using a Unaxis Shuttleline ICP RIE at constant process parameters of 10 sccm BCl_3, 10 sccm Ar, and 3 sccm N_2 flow, 550 W ICP power, 200 W RIE power, 2 mTorr pressure, and 23 °C temperature for 2 min. The etching rate was determined to be ~2 nm·s^{-1}. Electrical contacts were defined in two separate EBL steps, where Ni/Au (150/150 nm) and Ti/Al/Ti/Au (20/100/30/250 nm) were deposited for p-type shell and n-type core contacts, respectively. The contacts were annealed in nitrogen at 550 °C for 2 min. $I-V$ data were recorded using an Agilent semiconductor parameter analyzer (model 4156C) and EL spectra were recorded using a 300 mm spectrometer (150 lines·mm^{-1} grating) and a liquid nitrogen cooled charge-coupled device detector with a diode forward bias of 6 V. Standard solar illumination was provided by a Newport Solar Simulator (model 96000) with air mass global, AM 1.5G filter. UV light illumination was carried out using a Spectra Physics Q-switched 266 nm Nd:YVO_4 laser (model J40-BL6-266Q) with 35 kHz repetition rate, and 7 ns pulse duration. Illumination intensities were calibrated with a power meter (Coherent, Field Master).
(34) Shul, R. J.; McClellan, G. B.; Casalnuovo, S. A.; Rieger, D. J.; Pearton, S. J.; Constantine, C.; Barratt, C.; Karlicek, R. F.; Tran, C.; Schurman, M. *Appl. Phys. Lett.* **1996**, *69*, 1119.
(35) Luque, A.; Hegedus, S. *Handbook of PhotoVoltaic Science and Engineering*; Wiley: Chichester, 2003.
(36) Shah, J. M.; Li, Y. L.; Gessmann, T.; Schubert, E. F. *J. Appl. Phys.* **2003**, *94*, 2627.
(37) Wu, J.; Walukiewicz, W. *Superlattices Microstruct.* **2003**, *34*, 63.

NL900858V